A Ferromagnetic Interaction between Cu^{2+} Centers through a $[CrO_4]^{2-}$ Bridge: Crystal Structures and Magnetic Properties of $[\{Cu(acpa)\}_2(\mu\text{-}MO_4)]$ (M = Cr, Mo) (Hacpa = *N*-(1-Acetyl-2-propyridene)(2-pyridylmethyl)amine)

Hiroki Oshio,* Toshihiko Kikuchi, and Tasuku Ito

Department of Chemistry, Graduate School of Science, Tohoku University, Aoba-ku, Sendai 980-77, Japan

Received February 23, 1996[⊗]

The reaction of $[Cu(acpa)]^+$ with $[MO_4]^{2-}$ (Hacpa = *N*-(1-acetyl-2-propyridene)(2-pyridylmethyl)amine and M = Cr and Mo) in water−methanol or water−acetonitrile solution affords dinuclear copper(II) complexes with metalate bridges, $[\{Cu(acpa)\}_2(\mu\text{-}CrO_4)]\cdot 4CH_3OH\cdot 4H_2O$ (**1**) and $[\{Cu(acpa)\}_2(\mu\text{-}MoO_4)]\cdot 4H_2O$ (**2**), respectively. The crystal structures and the magnetic properties have been studied. Complexes **1** and **2** are isomorphous and the structures are made up of discrete dimers in which two copper(II) ions are bridged by the $[MO_4]^{2-}$ anion. The coordination geometry about the copper(II) ions is square planar with a N_2O chelate group from acpa and an oxygen atom from $[MO_4]^{2-}$. Magnetic susceptibility measurements for **1** revealed that a ferromagnetic interaction between copper(II) ions is propagated through the $[CrO_4]^{2-}$ bridge and the coupling constant ($2J$) was evaluated to be 14.6(1) cm^{-1} ($H = -2JS_1\cdot S_2$). In **2**, two copper(II) ions bridged by $[MoO_4]^{2-}$ anion are antiferromagnetically coupled with the $2J$ value of $-5.1(4)$ cm^{-1}. The ferromagnetic interaction in **1** is explained by means of the orbital topology of frontier orbitals. Crystal data: **1**, monoclinic, space group $P2_1/m$, $a = 8.349(2)$ Å, $b = 17.616(3)$ Å, $c = 10.473$ Å, $\beta = 107.40(2)°$, $Z = 2$; **2**, monoclinic, space group $P2_1/m$, $a = 8.486(2)$ Å, $b = 18.043(3)$ Å, $c = 9.753(2)$ Å, $\beta = 95.82(2)°$, $Z = 2$.

Introduction

Magnetochemistry of multinuclear metal complexes is a subject of current interest. The bridging ligands between paramagnetic metal ions usually mediate antiferromagnetic interactions due to the magnetic orbital overlap through the bridge. Ferromagnetic interactions, however, can be achieved, if the magnetic orbitals are (accidentally) orthogonal to each other.[1] For example, the orthogonality of dσ and dπ spins in Cu^{II}—V^{IV}═O and Ni^{II}—Cr^{III} complexes lead to the ferromagnetic interaction.[2,3] This approach has also been applied to metal complexes with organic radicals, in which the central metal ions are diamagnetic. In Ti^{IV}− and Ga^{III}−semiquinone complexes,[4] coordinated semiquinones are orthogonally arranged and the intramolecular ferromagnetic interactions -56 cm^{-1} ($H = JS_1\cdot S_2$) and 7.8 cm^{-1} ($H = -2JS_i\cdot S_j$) between semiquinones have been observed, respectively. In $[Cu^{I}(immepy)_2](PF_6)$ (immepy = bidentate iminonitroxide), a tetrahedral coordination geometry of the copper(I) ion gives an orthogonal arrangement of the iminonitroxides, which have ferromagnetic coupling with $2J$ value of 103 cm^{-1} ($H = -2JS_1\cdot S_2$).[5] On the other hand, tetraoxo anions such as phosphate, arsenate, vanadate, and molybdate have been known to interact and bridge metal ions. Diiron(III) complexes as models for purple acid phosphatases have been the subject of study from structural, electronic, and vibrational viewpoints.[6] However, magnetic interactions mediated through tetraoxo anions remain unclear. We report herein the structures and magnetic properties of dinuclear copper(II) complexes bridged by the tetraoxometalates, $[CrO_4]^{2-}$ and $[MoO_4]^{2-}$. The magnetic interaction through the metalate will be discussed by means of orbital symmetry of the frontier orbitals.

Experimental Section

Preparation of Complexes. Chemicals used were of reagent grade quality and were used without further purification. The ligand Hacpa was prepared by the literature method.[7]

$[\{Cu(acpa)\}_2(\mu\text{-}CrO_4)]\cdot 4CH_3OH\cdot 4H_2O$ (1). To a methanol solution (10 mL) of $Cu(BF_4)_2\cdot 4H_2O$ (310 mg, 1 mmol) and Hacpa (190 mg, 1 mmol) was added a water solution (3 mL) of triethylamine (200 mg, 2 mmol) and K_2CrO_4 (97 mg, 0.5 mmol). The solution was stirred at room temperature for 1 h, yielding a dark green solution. Upon standing in a refrigerator for 2 days, the mixture deposited dark green tablets. These were filtered, and one of these was subjected to the X-ray analysis. Some water and methanol molecules were lost upon drying. Anal. Calcd for $C_{20}H_{32}CrCu_2N_4O_9$ (**1**): C, 39.11; H, 4.77; N, 8.29. Found: C, 39.23; H, 4.92; N, 8.08.

$[\{Cu(acpa)\}_2(\mu\text{-}MoO_4)]\cdot 4H_2O$ (2). **2** was obtained in a manner similar to the preparation of **1** from a water−acetonitrile solution by using K_2MoO_4 (129 mg, 0.5 mmol) instead of K_2CrO_4. Some water and acetonitrile molecules were also lost upon drying. One of the dark blue tablets was subjected to X-ray analysis. Anal. Calcd for $C_{20}H_{32}Cu_2MoN_4O_9$ (**2**): C, 36.72; H, 4.48; N, 7.79. Found: C, 36.89; H, 4.53; N, 7.87.

[⊗] Abstract published in *Advance ACS Abstracts,* July 15, 1996.

(1) (a) Kollmar, C.; Kahn, O. *Acc. Chem. Res*. **1993**, *26*, 259. (b) Miller, J. S.; Epstein, A. J. *Angew. Chem. Int. Ed. Engl*. **1994**, *33*, 385.
(2) Kahn, O.; Galy, J.; Journaux, Y.; Jaud, J. Morgenstern-Badarau, I. *J. Am. Chem. Soc*. **1982**, *104*, 2165.
(3) Pei, Y.; Journaux, Y.; Kahn, O. *Inorg. Chem*. **1989**, *28*, 100.
(4) (a) Caneschi, A.; Dei, A.; Gatteschi, A. *J. Chem. Soc., Chem. Commun*. **1992**, 630. (b) Bruni, S.; Caneschi, A.; Cariati, F.; Delfs, C.; Dei, A.; Gatteschi, D. *J. Am. Chem. Soc*. **1994**, *116*, 1388. (c) Adams, D. M.; Rheingold, A. L.; Dei, A.; Hendrickson, D. N. *Angew. Chem., Int. Ed. Engl*. **1993**, *32*, 391.
(5) Oshio, H.; Watanabe, T.; Ohto, A.; Ito, T.; Nasgashima, U. *Angew. Chem., Int. Ed. Engl*. **1994**, *33*, 670.
(6) (a) Vincent, J. B.; Averill, B. A. *FASEB J*. **1990**, *4*, 3009. (b) Armstrong, W. H.; Lippard, S. J. *J. Am. Chem. Soc*. **1985**, *107*, 3730. (c) Drüeke, S.; Wieghard, K.; Nuber, B.; Weiss, J. *Inorg. Chem*. **1989**, *28*, 1414. (d) David, S. S.; Que, L., Jr. *J. Am. Chem. Soc*. **1990**, *112*, 6455. (e) Vincent, J. B.; Crowder, M. W.; Averill, B. A. *Biochemistry* **1992**, *31*, 3033. (f) Holz, R. C.; Elgren, T. E.; Pearce, L. L.; Zhang, J. H.; O'Connor, C. J.; Que, L., Jr. *Inorg. Chem*. **1993**, *32*, 5844.
(7) Oshio, H.; Toriumi, K.; Maeda, Y.; Takashima, Y. *Inorg. Chem*. **1991**, *30*, 4252.

S0020-1669(96)00204-2 CCC: $12.00

Table 1. Crystallographic Data of $[\{Cu(acpa)\}_2(\mu\text{-}CrO_4)]\cdot 4CH_3OH\cdot 4H_2O$ (**1**) and $[\{Cu(acpa)\}_2(\mu\text{-}MoO_4)]\cdot 4H_2O$ (**2**)

	1	**2**
formula	$C_{26}H_{50}CrCu_2N_4O_{14}$	$C_{22}H_{34}Cu_2MoN_4O_{10}$
fw	821.79	737.57
temp (°C)	-120	-60
cryst syst	monoclinic	monoclinic
space group	$P2_1/m$ (No. 11)	$P2_1/m$ (No. 11)
a (Å)	8.349(2)	8.486(2)
b (Å)	17.616(3)	18.043(3)
c (Å)	10.473(3)	9.753(2)
β (deg)	107.40(2)	95.82(1)
V (Å^3)	1469.7(6)	1485.6(6)
Z	2	2
ρ_{calcd} (g cm^{-3})	1.857	1.649
ρ_{obsd} (g cm^{-3})	1.87	1.63
μ(Mo Kα)(cm^{-1})	19.62	19.39
R^a	0.049	0.064
$R_w{}^b$	0.070	0.098

[a] $R = \sum(|F_o| - |F_c|)/\sum|F_o|$. [b] $R_w = [\sum w(|F_o| - |F_c|)^2/\sum w|F_o|^2]^{1/2}$ and $w = (\sigma_c^2 + (0.025x|F_o|)^2)^{-1}$.

Physical Measurement. EPR spectra were recorded on a JEOL FE2XG spectrometer operating at a X-band frequency with a magnetic field modulation of 100 kHz. Microwave frequency was measured with a Takeda Riken 5201 frequency counter, and magnetic field values of the signals were measured with an Echo Denshi EFM 200. UV−visible spectra were recorded on a Hitachi UV 340 spectrometer. Magnetic susceptibility data were collected in the temperature range 2.0−300 K and in an applied 1 T field with the use of a Quantum Design Model MPMS SQUID magnetometer. Powdered samples were contained in the small half of a gelatin capsule and a phenolic guide (clear soda straw) was used to house the sample holder and was fixed to the end of the magnetometer drive rod. $[Cr(NH_3)_6](NO_3)_3$ was employed as magnetometer calibrant. Pascal's constants were used to determinate the constituent atom diamagnetism.[8]

X-ray Crystallography. Crystals of $[\{Cu(acpa)\}_2(\mu\text{-}CrO_4)]\cdot 4CH_3OH\cdot 4H_2O$ (**1**) (dimensions 0.47 × 0.47 × 0.47 mm^3) and $[\{Cu(acpa)\}_2(\mu\text{-}MoO_4)]\cdot 4H_2O$ (**2**) (dimensions 0.66 × 0.15 × 0.15 mm^3) were used for data collection. A single crystal was mounted on a glass fiber with epoxy resin. Diffraction data were collected on a Rigaku 7S four-circle diffractometer equipped with graphite-monochromatized Mo Kα radiation (λ = 0.710 69 Å). Three standard reflections were measured every 200 data collections and revealed no fluctuation in intensities. The lattice constants were optimized from a least-squares refinement of the settings of 25 carefully centered Bragg reflections in the range $25° < 2\theta < 30°$. Empirical absorption corrections (ψ-scans) were carried out in each case. The maximum 2θ values for the data collection were 50° for **1** and 55° for **2**. The number of measured and unique reflections with R_{int} were 2845, 2661, and 0.022 for **1** and 3483, 3262, and 0.037 for **2**. The minimum and maximum transmission factors were 0.422 and 0.506 for **1** and 0.770 and 0.738 for **2**, respectively. Crystallographic data are collected in Table 1. The structures were solved by direct methods with SHELX-86[9] and Fourier techniques, and refined by full-matrix least-squares using XTAL 3.2.[10] All non-hydrogen atoms were readily located and refined with anisotropic thermal parameters. Hydrogen atoms for **1** were included in the refinement at calculated positions with C−H = 0.96 Å and U_H(iso) = 0.035 Å^2. Convergence was reached at R = 0.049 and R_w = 0.070 (the 2175 reflections with $I_0 > 3\sigma(I_0)$) for **1**, while the values for **2** were 0.064 and 0.098 (the 2390 reflections with $I_0 > 3\sigma(I_0)$). Final atomic parameters and equivalent isotropic thermal parameters for non-hydrogen atoms are listed in Tables 2 and SVII for **1** and **2**, respectively.

(8) *Theory and Application of Molecular Paramagnetism*; Boudreaux, E. A., Mulay, L. N., Eds.; Wiley and Sons, Inc.: New York, 1976.
(9) Sheldrick, G. M. *SHELXS-86*; University of Göttingen: Göttingen, Germany, 1986.
(10) Hall, S. R.; Sterwart, J. M. *XTAL3.2*; Universities of Western Australia and Maryland: Nedlands, Australia, and College Park, MD, 1992.

Table 2. Fractional Coordinates and Equivalent Isotropic Displacement Parameters (Å^2) of Non-hydrogen Atoms of $[\{Cu(acpa)\}_2(\mu\text{-}CrO_4)]\cdot 4CH_3OH\cdot 4H_2O$ (**1**)

	x/a	*y/b*	*z/c*	U^a
Cu	0.27313(7)	0.56712(3)	−0.00902(6)	0.0148(2)
Cr	0.1556(1)	3/4	0.0134(1)	0.0202(4)
O(1)	0.2773(4)	0.6722(2)	0.0403(4)	0.021(1)
O(2)	0.0288(8)	3/4	−0.1360(7)	0.054(3)
O(3)	0.0477(8)	3/4	0.1180(8)	0.047(3)
O(4)	0.3468(4)	0.5958(2)	−0.1574(3)	0.020(1)
O(5)	0.4498(8)	3/4	−0.1670(7)	0.042(3)
O(6)	0.3040(7)	1/4	0.2830(6)	0.039(2)
O(7)	0.534(1)	1/4	0.606(1)	0.120(6)
O(8)	0.048(2)	3/4	−0.474(2)	0.146(9)
N(1)	0.1909(5)	0.5344(2)	0.1415(4)	0.017(1)
N(2)	0.2686(5)	0.4604(2)	−0.0474(4)	0.018(1)
C(1)	0.1547(6)	0.5797(3)	0.2324(5)	0.021(2)
C(2)	0.0917(7)	0.5514(3)	0.3294(5)	0.025(2)
C(3)	0.0645(7)	0.4747(3)	0.3346(5)	0.027(2)
C(4)	0.1017(7)	0.4276(3)	0.2422(6)	0.024(2)
C(5)	0.1662(6)	0.4592(3)	0.1473(5)	0.020(2)
C(6)	0.2183(6)	0.4116(3)	0.0461(5)	0.019(2)
C(7)	0.3096(6)	0.4286(3)	−0.1471(5)	0.019(2)
C(8)	0.3607(6)	0.4716(3)	−0.2420(5)	0.023(2)
C(9)	0.3733(6)	0.5496(3)	−0.2450(5)	0.020(2)
C(10)	0.3040(6)	0.3437(3)	−0.1625(6)	0.024(2)
C(11)	0.4208(7)	0.5873(3)	−0.3574(5)	0.028(2)
C(12)	0.369(1)	1/4	0.541(1)	0.109(8)
C(13)	−0.039(2)	0.6846(7)	−0.498(1)	0.122(8)

[a] Equivalent isotropic U defined as one-third of the trace of the orthogonalized $\mathbf{U}_{ij}$ tensor.

Table 3. Selected Bond Distances (Å) and Angles (deg) of $[\{Cu(acpa)\}_2(\mu\text{-}CrO_4)]\cdot 4CH_3OH\cdot 4H_2O$ (**1**)

Cu−O1	1.919(4)	Cu−O4	1.903(4)
Cu−N1	1.984(5)	Cu−N2	1.921(4)
Cr−O1	1.679(4)	Cr−O2	1.606(6)
Cr−O3	1.614(8)	Cu−Cr	3.3961(9)
Cu−Cu*	6.443(1)		
O1−Cr−O2	110.7(2)	O1−Cr−O3	108.6(2)
O1−Cr−O1*	109.5(2)	O2−Cr−O3	108.8(4)
O1−Cu−O4	88.8(2)	O1−Cu−N1	92.8(2)
O1−Cu−N2	176.5(2)	O4−Cu−N1	177.9(1)
O4−Cu−N2	94.6(2)	N1−Cu−N2	83.8(2)
Cu−O1−Cr	141.3(2)		

[a] Key to symmetry operation: (*) x, 3/2 − y, z.

Table 4. Selected Bond Distances (Å) and Angles (deg) of $[\{Cu(acpa)\}_2(\mu\text{-}MoO_4)]\cdot 4H_2O$ (**2**)

Mo−O1	1.782(6)	Mo−O2	1.73(1)
Mo−O3	1.730(9)	Cu−O1	1.929(6)
Cu−O4	1.907(6)	Cu−N1	1.979(7)
Cu−N2	1.917(8)	Mo−Cu	3.576(1)
Cu−Cu*	6.703(2)		
O1−Mo−O2	109.8(3)	O1−Mo−O3	108.7(2)
O1−Mo−O1*	111.2(3)	O2−Mo−O3	108.7(5)
O1−Cu−O4	87.4(3)	O1−Cu−N1	93.8(3)
O1−Cu−N2	176.0(3)	O4−Cu−N1	178.5(3)
O4−Cu−N2	95.1(3)	N1−Cu−N2	83.6(3)
Mo−O1−Cu	149.0(4)		

[a] Key to symmetry operation: (*) x, 3/2 − y, z.

Results and Discussions

Description of the Structures. $[\{Cu(acpa)\}_2(\mu\text{-}CrO_4)]\cdot 4CH_3OH\cdot 4H_2O$ (1) and $[\{Cu(acpa)\}_2(\mu\text{-}MoO_4)]\cdot 4H_2O$ (2). Complexes **1** and **2** crystallize in the monoclinic system with space group $P2_1/m$. Selected bond distances and angles are listed in Tables 3 and 4, respectively, and an ORTEP view of **1** is presented in Figure 1 with the atom numbering scheme. The numbering system for **2** is the same as that used in **1** except for the Mo atom. The complex molecules of **1** and **2** are located

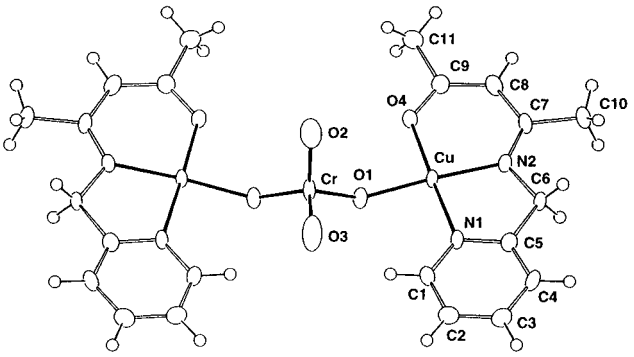

Figure 1. ORTEP drawing of [{Cu(acpa)}$_2$(μ-CrO_4)] (**1**).

on a crystallographic mirror plane; thus the asymmetric unit consists of a half-molecule. Copper(II) ions in each asymmetric unit are bridged by the O1−M−O1* unit of $[MO_4]^{2-}$ (M = Cr or Mo) with separations of 6.443(1) and 6.703(2) Å, respectively. The coordination geometry about the copper(II) ions is square planar, in which the four coordination sites are occupied with N_2O chelate groups from acpa and an oxygen atom from the $[MO_4]^{2-}$ anion. The copper(II) ions in **1** and **2** stay 0.03(1) Å above the mean plane of N1−N2−O1−O4 and bond distances between the copper(II) and coordinated atoms are 1.903(4)−1.984(5) Å, which implies that the magnetic orbital of the copper(II) ion is $d_{x^2-y^2}$. Two square planar coordination planes of the copper(II) ions bridged by the $[CrO_4]^{2-}$ and $[MoO_4]^{2-}$ unit make angles of 10.6(1) and 4.8(2)°, respectively. The coordination geometries around the Cr and Mo atoms are pseudotetrahedral, where M−O (M = Cr and Mo) bond lengths are in the range 1.606(6)−1.679(4) and 1.730(9)−1.782(6) Å with O−M−O bond angles of 108.6(2)−110.7(2) and 108.7(2)−111.2(3)°, respectively. The bond length of Cr or Mo with the O1 atoms coordinated to the copper(II) ion is the longest among the M−O bonds and the bond angles (Cr−O1−Cu and Mo−O1−Cu) about the bridging O1 atom are 141.3(2) and 149.0(4)°, respectively.

Magnetic Properties. Temperature dependent magnetic susceptibilities for the complexes have been measured down to 2.0 K and $\chi_m T$ values vs temperature for **1** and **2** are plotted together in Figure 2, where χ_m is the molar magnetic susceptibility per dinuclear unit.

For **1**, the χ_mT value at 300 K is 0.89 emu mol^{-1} K, which would be expected for the uncorrelated spins. When the temperature is lowered, $\chi_m T$ for **1** increases and exhibits a maximum at 10 K ($\chi_m T$ = 1.00 emu mol^{-1} K) and then decreases. The magnetic behavior for **1** suggests that a ferromagnetic interaction between the copper(II) ions is predominant at intermediate temperature and then a weaker antiferromagnetic coupling is involved at lower temperature. The magnetic susceptibility data were analyzed by the Bleaney−Bowers equation ($H = -2JS_1 \cdot S_2$) as[11]

$$\chi_m = \frac{Ng^2\beta^2}{k(T-\Theta)}\left[\frac{2}{3+\exp(-2J/kT)}\right] + N\alpha \qquad (1)$$

where the contribution of the intermolecular antiferromagnetic interaction (Θ) and temperature independent term ($N\alpha$: 60 × 10^{-6} emu/Cu) were included in the calculations. The symbols have their usual meaning. The best fit parameters were $2J$ = +14.6(1) cm^{-1}, g = 2.12(1), and Θ = −0.8(1) K. In contrast to **1**, the $\chi_m T$ values for **2** show gradual decrease as the temperature was lowered, and this behavior is characteristic of antiferromagnetically coupled copper(II) ions. The least square fitting of the experimental data with the equation (1) led to $2J$ = −5.1(4) cm^{-1}, g = 2.07(1), and Θ = −1.2(1) K. An EPR measurement for **1** showed no signal at 77 K, which might be due to a rapid spin relaxation. On the other hand, **2** showed an axially symmetric EPR pattern ($g_{\|}$ = 2.195 and $g_{\perp}$ = 2.079) at 77 K, which is characteristic of magnetically isolated copper(II) ions with square planar coordination.

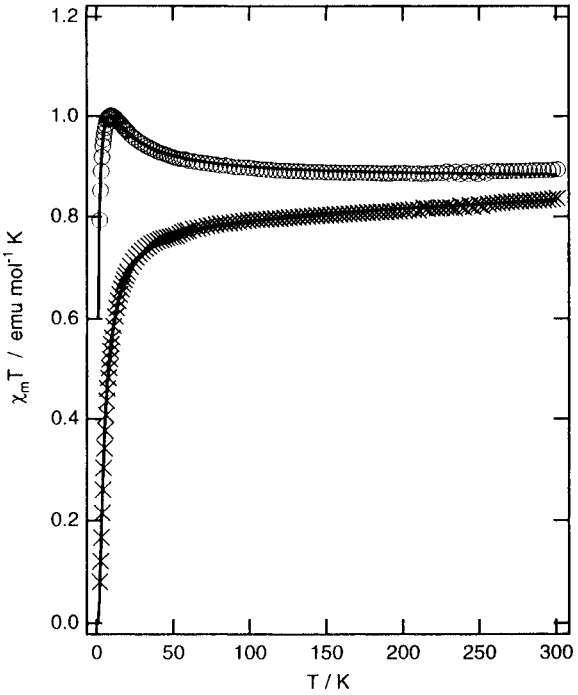

Figure 2. Plots of $\chi_m T$ *vs* T for (○) [{Cu(acpa)}$_2$(μ-CrO_4)]·4CH_3OH·4H_2O (**1**) and (×) [{Cu(acpa)}$_2$(μ-MoO_4)]·4H_2O (**2**). Solid lines correspond to the best fit curves by using the parameters given in the text.

When two magnetic orbitals, each having one electron, are sufficiently close to interact, either a ferromagnetic or an antiferromagnetic interaction is propagated. The magnetic interaction can be expressed as the sum of K (exchange integral) and $2\beta S$ (β, transfer integral, and S, overlap integral) which favor the ferromagnetic and antiferromagnetic interactions, respectively.[1] When two magnetic orbitals overlap each other, the $2\beta S$ term is much larger than the K term, and thus the antiferromagnetic interaction is predominant. On the other hand, in the case of the two magnetic orbitals being orthogonal to each other (strict orthogonality) or the $2\beta S$ term being small enough compared with the K term, the ferromagnetic interaction can be obtained. It should be noted that bridging ligands are responsible for the ferromagnetic contribution and that magnetic properties can be understood by orbital symmetry of the bridging ligand and magnetic orbitals.

If we assume that the ions $[CrO_4]^{2-}$ and $[MoO_4]^{2-}$ have tetrahedral geometry, where the X-ray crystallographic analyses for **1** and **2** revealed the two ions to have pseudotetrahedral symmetry, we expect that the metal d-orbitals are split into e and t_2 type orbitals and p-orbitals of the coordinated oxygen atoms forms a_1 and t_2 type orbitals. The e pair of the d-orbitals has no matching combination of oxygen orbitals, hence these orbitals remain nonbonding. The t_2 type orbitals of the metal ion, however, form triply degenerate bonding and antibonding orbitals with those of the oxygen p-orbitals and six electrons form the coordinated oxygen p-orbitals occupy the t_2-type bonding orbitals (Figure 3a). When the $[CrO_4]^{2-}$ anion bridges copper(II) ions along the equatorial directions, two of the t_2

(11) Bleaney, B.; Bowers, K. D. *Proc. R. Soc. London, A* **1952**, *214*, 451.

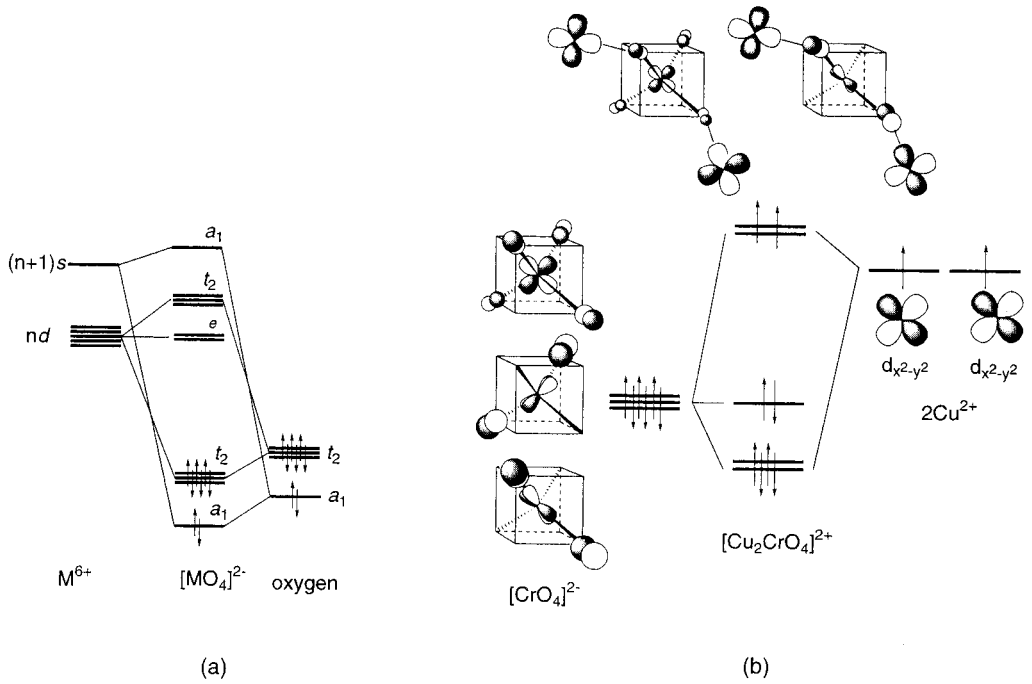

Figure 3. (a) Molecular orbital scheme of the $[CrO_4]^{2-}$ anion under T_d symmetry and (b) a proposed molecular orbital scheme for the $[Cu_2CrO_4]^{2+}$ chromophore, where the occupied t_2 type orbitals of $[CrO_4]^{2-}$ form quasi doubly-degenerate molecular orbitals with $d_{x^2-y^2}$ orbitals.

type molecular orbitals of the $[CrO_4]^{2-}$ anion form two sets of σ-type bonding and antibonding orbitals with $d_{x^2-y^2}$ orbitals of the copper(II) ions, and the remainder of the t_2 type orbitals remain nonbonding. The two unpaired electrons from the copper(II) ions occupy the antibonding orbitals (Figure 3b). In **1**, the complex molecule has only mirror symmetry; hence the molecular geometry of the complex is C_s. It should be noted that there are no degenerate orbitals under the C_s symmetry. The magnetic susceptibility measurement of **1**, however, does show the ferromagnetic interaction between the copper(II) ions. Therefore, the two antibonding MOs must be energetically close enough to have a large exchange integral K overcoming the stabilization of the singlet state, or they must be nearly degenerate. In contrast to **1**, **2** showed only a weak antiferromagnetic interaction through the $[MoO_4]^{2-}$ ion. The lack of the substantial magnetic interaction in **2** can be understood by orbital energy mismatch of the Mo and O atoms. The UV−visible spectrum of K_2CrO_4 in water shows strong absorption bands at 370 ($\epsilon = 3900$ M^{-1} cm^{-1}) and 270 nm ($\epsilon = 3200$ M^{-1} cm^{-1}) which are assigned to LMCT bands from O to Cr atom.[12] The corresponding CT bands for K_2MoO_4 appear in the high energy region (226 nm with $\epsilon = 5000$ M^{-1} cm^{-1} and 207 nm with $\epsilon = 9800$ M^{-1} cm^{-1}).[13] The UV-visible spectra suggest that in the $[CrO_4]^{2-}$ ion the t_2 type orbitals undergo substantial mixing of the chromium d- and oxygen p-orbitals, while such orbital mixing for $[MoO_4]^{2-}$ is energetically inaccessible. In **1** and **2**, the oxygen atoms of the metalate ions coordinate to the copper(II) ions from their equatorial plane ($d_{x^2-y^2}$ orbital) and the spin of the copper(II) ions is considered to be delocalized onto the coordinated oxygen atoms of the metalate ions. In the $[MoO_4]^{2-}$-bridged complex, however, the magnetic interactions between two delocalized spins on the oxygen atoms are disconnected by the Mo atom due to the energy mismatching of the molybdenum d- and oxygen p-orbitals. Hence, the fairly weak antiferromagnetic interaction observed in **2** does not occur through $[MoO_4]^{2-}$ unit but results from the magnetic dipole−dipole interaction.

Conclusion

One of the purposes of this paper was to verify the validity of the $[CrO_4]^{2-}$ bridging unit to link paramagnetic species with ferromagnetic interactions. The chromate bridged dicopper system studied here does show the ferromagnetic interaction due to the accidental degeneracy of the σ-type frontier orbitals. Some multinuclear complexes with $[CrO_4]^{2-}$ as the bridging ligand have been magnetically and structurally characterized.[14] For example, $[LFe^{III}(\mu\text{-}CrO_4)_3Fe^{III}L]$ (L = 1,4,7-trimethyl-1,4,7-triazacyclononane) has shown an antiferromagnetic interaction ($2J = -15$ cm^{-1}) between the high-spin iron(III) centers through the three chromate bridges.[15] The antiferromagnetic interaction in the iron(III) complexes might be understood by an extra π-orbital overlap between $[CrO_4]^{2-}$ and Fe^{III} ions leading to the nondegenerate frontier orbitals of the $[Fe^{III}_2(\mu\text{-}CrO_4)_3]$ chromophore.

Acknowledgment. This work was in part supported by a Grant-in-aid for Scientific Research (No. 08640705) from the Ministry of Education, Science, and Culture, Japan.

Supporting Information Available: Tables SI−SX, listing X-ray data collection parameters, derived hydrogen positions, thermal parameters, and bond distances and angles and ORTEP figures (15 pages). Ordering information is given on any current masthead page.

IC960204+

(12) (a) Duiker, J. C.; Ballhausen, C. J. *Theor. Chim. Acta* **1968**, *12*, 325. (b) Johnson, L. W.; McGlynn, S. P. *Chem. Phys. Lett.* **1970**, *7*, 618. (c) Miller, R. M.; Tinti, D. S.; Case. D. A. *Inorg. Chem.* **1989**, *28*, 2738.

(13) Müller, A.; Diemann, E. *Chem. Phys. Lett.* **1971**, *9*. 369.

(14) (a) Harel, M.; Knobler, C.; McCullough, T. D. *Inorg. Chem.* **1969**, *8*, 11. (b) Gatehouse, B. M.; Guddat, L. W. *Acta Crystallogr., Sect. C: Cryst. Struct. Commun.* **1987**, *C43*, 1445. (c) Bensch, W.; Seferiadis, N.; Oswald, H. R. *Inorg. Chim. Acta* **1987**, *126*, 113.

(15) Chaudhuri, P.; Winter, M.; Wieghardt, K.; Gehring, S.; Haase, W.; Nuber, B.; Weiss, J. *Inorg. Chem.* **1988**, *27*, 1564.